(2)

NRL Memorandum Report 5467

AD-A148 698

Simulation of Repetitively-Pulsed Laser Irradiation of Graphite-Epoxy Composite

G. P. MUELLER

Radiation-Matter Interactions Branch
Condensed Matter and Radiation Sciences Division

20000803193

December 12, 1984

NAVAL RESEARCH LABORATORY
Washington, D.C.

AD-A148698

SECURITY CLASSIFICATION OF THIS PAGE

REPORT DOCUMENTATION PAGE

1a REPORT SECURITY CLASSIFICATION UNCLASSIFIED	1b RESTRICTIVE MARKINGS
2a SECURITY CLASSIFICATION AUTHORITY	3 DISTRIBUTION/AVAILABILITY OF REPORT Approved for public release; distribution unlimited.
2b DECLASSIFICATION/DOWNGRADING SCHEDULE	
4 PERFORMING ORGANIZATION REPORT NUMBER(S) NRL Memorandum Report 5467	5 MONITORING ORGANIZATION REPORT NUMBER(S)
6a NAME OF PERFORMING ORGANIZATION Naval Research Laboratory 6b OFFICE SYMBOL (If applicable) Code 6650	7a NAME OF MONITORING ORGANIZATION
6c ADDRESS (City, State, and ZIP Code) Washington, DC 20375-5000	7b ADDRESS (City, State, and ZIP Code)
8a NAME OF FUNDING/SPONSORING ORGANIZATION 8b OFFICE SYMBOL (If applicable)	9 PROCUREMENT INSTRUMENT IDENTIFICATION NUMBER
8c ADDRESS (City, State, and ZIP Code)	10 SOURCE OF FUNDING NUMBERS PROGRAM ELEMENT NO: 62761N; PROJECT NO:; TASK NO:; WORK UNIT ACCESSION NO: DN780-081

11 TITLE (Include Security Classification)
Simulation of Repetitively-Pulsed Laser Irradiation of Graphite-Epoxy Composite

12 PERSONAL AUTHOR(S)
Mueller, G.P.

13a TYPE OF REPORT	13b TIME COVERED	14 DATE OF REPORT (Year, Month, Day)	15 PAGE COUNT
Interim	FROM TO	1984 December 12	32

16 SUPPLEMENTARY NOTATION

17 COSATI CODES			18 SUBJECT TERMS (Continue on reverse if necessary and identify by block number)
FIELD	GROUP	SUB-GROUP	Pulsed lasers; Laser irradiation simulation; Graphite-epoxy composite

19 ABSTRACT (Continue on reverse if necessary and identify by block number)

The CW laser irradiation code of Griffis, Masumura and Chang was modified to simulate pulsed laser irradiations. Extensive changes were required to cure the numerical instabilities produced in the code by the high peak powers common to pulsed lasers. The new code was tested against the original Griffis, Masumura and Chang code and against a simple heat capacity model. A comparison was made with some of the experimental pulsed irradiations of Cozzens, et al, resulting in doubts about the accuracy of the model for the thermal properties of the graphite-epoxy under rapid heating.

20 DISTRIBUTION/AVAILABILITY OF ABSTRACT	21 ABSTRACT SECURITY CLASSIFICATION
☒ UNCLASSIFIED/UNLIMITED ☐ SAME AS RPT ☐ DTIC USERS	UNCLASSIFIED
22a NAME OF RESPONSIBLE INDIVIDUAL G. P. Mueller	22b TELEPHONE (Include Area Code) (202) 767-2972
	22c OFFICE SYMBOL Code 6650

DD FORM 1473, 84 MAR — 83 APR edition may be used until exhausted; all other editions are obsolete

SECURITY CLASSIFICATION OF THIS PAGE

CONTENTS

INTRODUCTION 1

THE TIME EVOLUTION MESH 2

THE MESH FOR PENETRATION DEPTH 4

NEW ITERATION METHOD DURING ABLATION 4

NEW METHOD FOR REPRESENTING THERMAL PROPERTIES 6

SIMPLE HEAT CAPACITY TEST 12

COMPARISON WITH THE GRIFFIS, MASUMURA, AND CHANG CALCULATION 14

SAMPLE CALCULATION FOR A REPETITIVELY-PULSED IRRADIATION 16

COMPARISON WITH EXPERIMENTAL REPETITIVELY-PULSED IRRADIATIONS 19

CONCLUSIONS 22

ACKNOWLEDGMENTS 23

REFERENCES 24

APPENDIX A: THERMAL PROPERTIES OF THE GRAPHITE EPOXY COMPOSITE ... 25

APPENDIX B: CUMULATIVE HEAT CAPACITY 27

Simulation of Repetitively-Pulsed Laser Irradiation of Graphite-Epoxy Composite

1. INTRODUCTION

For their investigations of the rapid heating of graphite epoxy composites, Griffis, Masumura and Chang (GMC) [1] developed a computer code to calculate the response of a composite to CW laser irradiations with fluences of the order of kilowatts per square centimeter. Data are also available for the repetitively-pulsed laser irradiations of the same composite material. These irradiations involve much higher peak powers, of the order of megawatts per square centimeter, typically with 100 pulses of 10 μs duration at the rate of 100 pulses per second. The average energy deposited (100×10^{-5} s $\times 10^{6}$ W/cm^2 = 10^3 J/cm^2) is about the same as in the GMC work.

In this report I describe the modifications that I made to the GMC code so as to handle the larger pulsed fluences. When attempting to use the GMC code at higher fluences, several problems arose. The code had to be modified to handle pulsed irradiations, but this did not, in itself, disturb the numerical procedures used in the code. The next section describes the new time-mesh structure, which allows a repeated heat-on/heat-off irradiation. The three order-of-magnitude increase in the peak fluence did generate numerical problems. Due to the low thermal conductivity of the composite material, enormous thermal gradients are created at the surface of the material--gradients of the order of 10^7-10^8°C/cm. This problem was circumvented by replacing the grid sturcture for the depth variable with another structure that has a very fine mesh size at the surface and that gradually coarsens as one goes deeper into the material. This mesh is described in Section 3.

Manuscript approved August 21, 1984.

In the GMC model of the composite response at high temperature, the material (graphite and residual epoxy) decomposes at 3316°C. Once the front surface reaches this temperature, the surface begins to recede. GMC modified the equations describing the surface conditions in order to simulate this recession. At the higher fluences used with the repetitively-pulsed irradiations, their procedure becomes numerically unstable. I describe in Section 4 a modified method for handling the recession.

Section 5 describes the changes made in the handling of the thermal properties, which has the effect of both improving the numerical convergence of the calculations and improving their accuracy. The following section reports a test of the code that compares the program's calculation of the time for a complete burnthrough with the time derived from simple heat capacity estimates.

In order to verify that none of the changes outlined above made any substantial change in the low fluence, CW results, Section 7 compares one of the calculations made by GMC to the same calculation made with the modified code. The next section contains a sample calulation for a pulsed irradiation. Section 9 then presents a detailed comparison of this code's results with an experimental pulsed irradiation.

Throughout this report we follow the notation of Griffis, Masumura and Chang. Rather than repeat equations that appear in their report, we will refer to them directly by using their equation numbers prefaced by a "G". We also follow GMC in using the expressions for surface losses due to convection and reradiation that are given by Hobbs, et al [2]. The concluding section will emphasize the need for better measurements of the thermal properties of the composite.

2. THE TIME EVOLUTION MESH

We describe the structure of the a pulsed irradiation by three time periods: t_1, the length of an individual laser pulse; t_2, the time between pulses; and t_3, the length of time the code is allowed to run at

the end of the irradiation. Thus the total time simulated by the code is

$$t = n_p (t_1 + t_2) + t_3 \qquad (1$$

where n_p is the number of pulses. Typically, an experimental run will consist of 100 pulses at 100 pps, with 10 μs pulse lengths, for which case we have t_1=10 μs, t_2=9990 μs, and n_p=100. Having set these intervals, we break them into n_1, n_2, and n_3 subintervals,

$$t_s = t_{s1} + t_{s2} + \ldots + t_{sn_s}, \qquad (2$$

so that there are a total of n_t time intervals, where

$$n_t = n_p (n_1 + n_2) + n_3 . \qquad (3$$

The code is most unstable, numerically, at the beginning of a pulse--the thermal gradients are largest then and the difficulties associated with the abrupt changes in the composite's thermal properties [1] are worst. Consequently, the code requires small time intervals at the beginning of a pulse. Later, after the heat has flowed into the interior of the composite and after the temperature has risen above the region (200-500°C) where the thermal properties are changing rapidly, larger time intervals can be used. We satisfiy the requirements by setting the time steps for the pulse period as

$$t_{1i} - t_{1i-1} = t_1 \frac{\exp(i\, a_1) - \exp((i-1)\, a_1)}{\exp(n_1\, a_1) - 1}, \quad i=1,2\ldots n \qquad (4$$

with similar expressions for the other time intervals. The values of a_1, a_2, and a_3 can be set as desired; typical values are a_1 = 0.07, a_2 = 0.10, and a_3 = 0.10, in which case, if t_1=10 μs, n_1=100, t_2=9.99 ms, and n_2=100, the first time step is 0.66 ns long, the 100th is 0.68 μs, the 101st is 48 ns, and the 200th is 0.95 ms. The form (4) is flexible, allowing great disparity in the time steps, as above, and allowing equal steps as the a_i go to zero.

In the course of its calculations, if the code runs into numerical difficulty during a particular time step, such as the non-convergence of one of the iteration procedures, then the size of that time step is halved and the procedure restarted. Once the whole time step has been worked through, the program reverts to the original time step sequence. This self adjusting feature makes the code more flexible, so that larger and more efficient time steps can be used most of the time; shorter time steps are used only when necessary.

3. THE MESH FOR PENETRATION DEPTH

When a several megawatt irradiation first impinges on the composite material, thermal gradients of the order of 10^7-10^8°C/cm are seen. In order that the calculated temperatures not vary too much from gird point to adjacent gird point, it is necessary that the mesh be quite fine near the surface. To accomplish this we again use the expcnential form

$$x_0 = C$$
$$x_i = L\,[\exp(i\,b) - 1) \,/\, (\exp(n_m\,b) - 1]\ ,\ i=1,2...n_m \qquad (5$$

where L is the thickness of the material and n_m is the initial number of mesh points. Typically, we use a value of b=0.035, so that for a thickness of 0.254 cm the first grid slab has a thickness of $4X10^{-8}$ cm and the final slab a thickness of $9X10^{-3}$ cm.

4. NEW ITERATION METHOD DURING ABLATION

The equations governing the response of the composite change once the front surface of the composite reaches the ablation temperature. The equation [1] relating the surface temperatures and the recession velocity is Eq. (G15), which we reproduce here

$$T_{1j} + T_{1j+1} - T_{2j} - T_{2j+1} =$$

$$= C_f [2z_2 k^2 - \rho C_p k V_m z_2^2 - C_f (dk/dT) z_2^2] k^{-3} \quad (6$$

$$C_f = Q - \rho H_s V_m \ , \quad (7$$

where Q is the absorbed power flux less the surface losses. (The second C_f factor in Eq. (6) was inadvertently left out of Eq. (15) of Ref. (1).)

Griffis, Masumura and Chang set the front surface temperature during ablation to be

$$T_{1j} = T_{1j+1} = T_s \ . \quad (8$$

They then solve the coupled equations for the new set of temperatures $[T_{ij+1}, i=2,\ldots,n_m]$, and then use Eq. (G15) (with $T_{1j} = T_{1j+1} = T_s$) to determine V_m. They then iterate using the new V_m and T_{ij+1} values. This process is repeated until successive values of V_m are within 2 percent of each other.

When I attempted to use their iteration scheme with higher fluences (2 MW/cm^2), the code became unstable, so I created a modified interation method based on the same equations. Instead of Eq. (8), I used Eq. (7) as one of the n_m equations linking the temperatures at the n_m grid points. The procedure is started by guessing at a value for V_m. After the new set of temperatures $[T_{ij+1}, i=1,2,\ldots,n_m]$ is calculated, the surface temperature T_{1j+1} is checked to see if it is within a prescribed neighborhood of T_s. If so, the calculation for that time step is finished. If not, the new temperatures are scaled

$$T'_{ij+1} = (T_s / T_{1j+1}) T_{ij+1} \quad (9$$

and a new guess is made as to the value of V_m. This procedure is repeated until a given V_m yields T_{1j+1} within the prescribed neighborhood of T_s.

5. NEW METHOD FOR REPRESENTING THERMAL PROPERTIES

The thermal properties we use in these calculations are those given in Menousek and Monin [3]. The density, specific heat, and thermal conductivity are represented by a series of ramp and step functions; the low energy portions of these properties are pictured in the following figures.

Figure 1 depicts the Menousek and Monin characterization of the specific heat of the graphite epoxy as it is heated from 0°C to 900°C. The large changes in the specific heat between 340°C and 510°C reflect the chemical changes that the epoxy undergoes between these temperatures. What remains above 510°C are the graphite fibers and, presumably, some residue of the pyrolyzed epoxy. Although it is not completely shown in Figure 1, there is a gentle rise of the specific heat between 510°C and 3316°C where the graphite fibers and epoxy residue sublimate. We have used the Menousek and Monin values for the specific heat, with one modification. Once the composite has been heated above 510°C the epoxy is permanently lost, so thereafter the specific heat is represented by the line from 510°C to 3316°C extended down to 0°C; the extension is shown by the large-dash curve in Fig. (1). Also shown in this figure is the characterization used by GMC, which consists of the Menousek and Monin curves with the steeper ramps replaced by gentler ones. We will discuss this point further after displaying the other properties.

Figure 2 shows the Menousek and Monin version of the density up to 900°C; it is constant above 510°C. We again use their version upon first heating the composite. Once the material has been heated above 510°C we assume a constant value of the density of 1.084 g/cm^3. The slightly modified GMC version for the density is also shown in the figure. The same discussion applies to Figure 3, showing the thermal conductivity, with one exception. The Menousek and Monin curve is a straight line dropping from a value of 1.452 W/cm°C at 10°C to a value 0.173 W/cm°C at 538°C, after which it is constant at that value. For convenience, we shifted the position at which the curve turns from 538°C to 510°C, the same temperature at which the other properties break. Given the uncertainties with which these properties are known [3], this seems a negligible change. All of the properties that

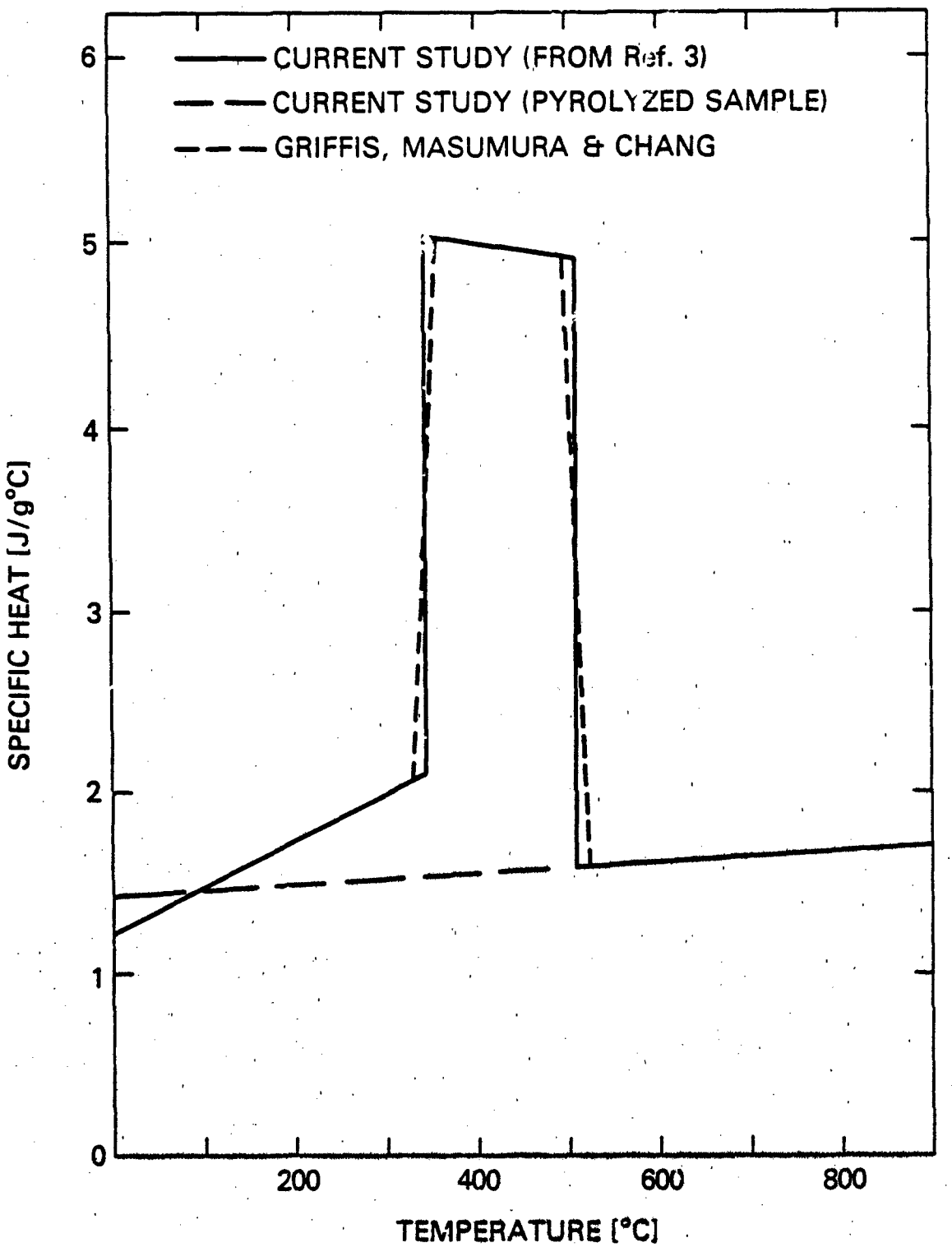

Fig. 1 -- Specific Heat of the graphite epoxy. Shown is the original Menousek and Monin version, which is used in the current study, and the slightly modified version used by GMC. Also shown is the form used in this study when the sample has been heated enough to pyrolyze the epoxy.

have been presented graphically in this section are given in tabular form in Appendix A.

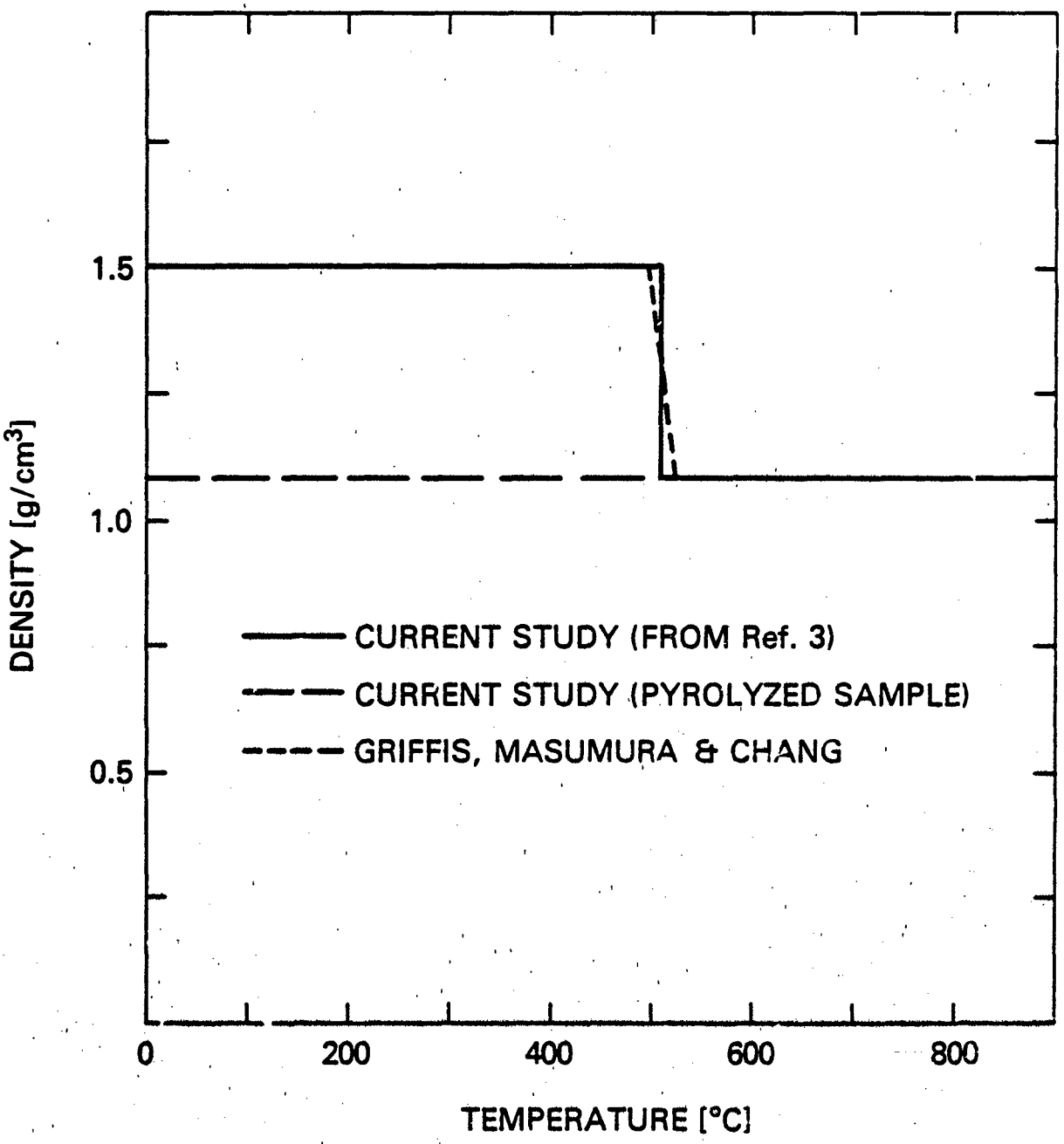

Fig. 2 -- The density of the graphite epoxy. Shown is the original Menousek and Monin version, which is used in the current study, and the slightly modified version used by GNC. Also shown is the form used in this study when the sample has been heated enough to pyrolyze the epoxy.

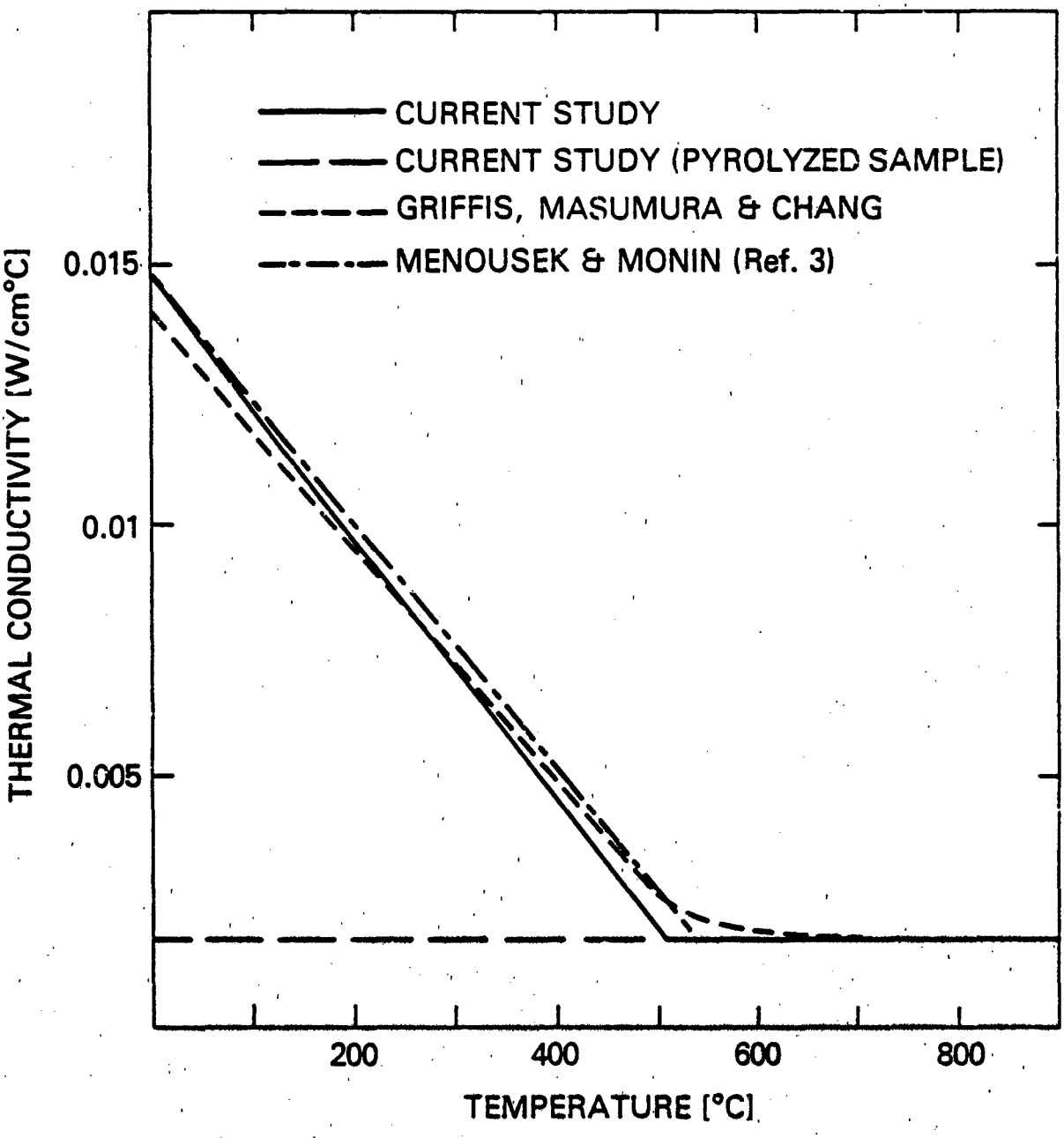

Fig. 3 -- The thermal conductivity of the graphite epoxy. Shown is the version used in this study and the version used by GMC, both of which are slightly modified forms of the original Menousek and Monin version. Also shown is the form used in this study when the sample has been heated enough to pyrolyze the epoxy.

We conclude this section on thermal properties by describing an improved method of utilizing these properties within the code. The original GMC code supplies thermal properties in the following manner during a given time interval: For each grid step of the spatial coordinate, there is an initial temperature T_j and an estimated final temperature T_2. The GMC code averages these two temperatures and then supplies the thermal properties corresponding to the average temperature by interpolating in Table A3. A more accurate method of supplying the thermal properties is to provide the average thermal properties over the temperature range T_j to T_2. As an example, we will use

$$K = \frac{1}{T_2 - T_j} \int_{T_j}^{T_2} dT\, K(T) \qquad (10$$

rather than using the thermal conductivity at the average temperature $(T_j+T_2)/2$.

Because T_2 varies with each iteration, if one of the temperatures lies near one of the snarper boundaries shown in Figures 1-3, then minor shifts in the temperature can make significant shifts in the reported thermal properties. This effect tends to destablize the convergence of the iteration procedure.

In Figure 4 we show an example of the benefit of the improved method; the specific heat is plotted as a function of T_2 while T_j is fixed at 490°C. In this example, there is as much as a ten percent error in C_p at T_2=530°C ($(T_2+T_j)/2$ = 510°C). (Even larger errors occur in this example when T_2=560°C, but usually the time steps are picked so that this large a change in temperature would not arise.) In the same vein, the derivative of the diffusivity, which appears in Eq. (6), has discontinuities as one crosses some of the boundary points. The GMC method of supplying the average value of this quantity also yields discontinuities. These discontinuities can lead to minor instablities in the iteration process, requiring a greater number of iterations and producing less accuracy in the final results. The new method described in this section provides a smoother and a more realistic averaging process.

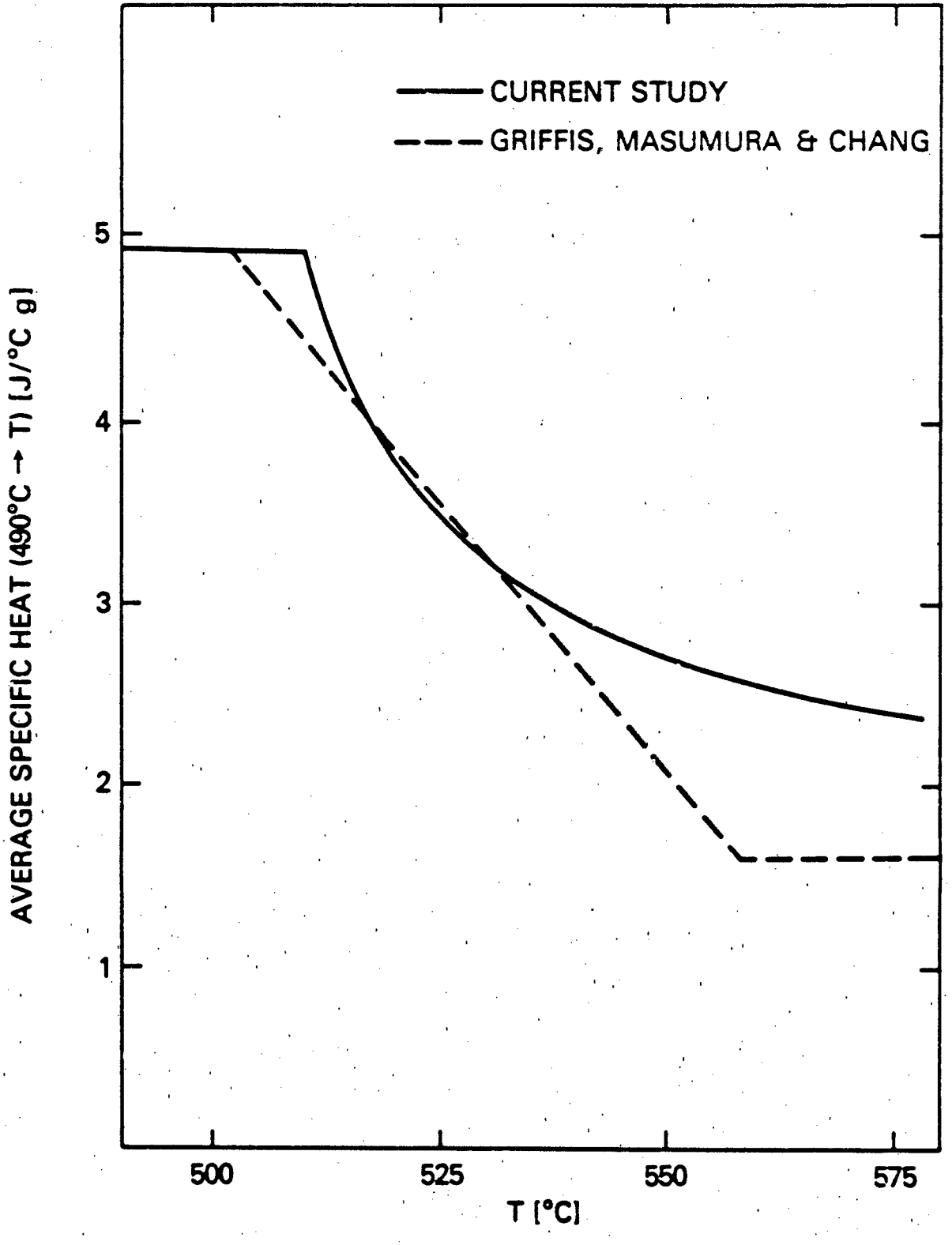

Fig. 4 -- An example of the specific heat as supplied by the current study and by GMC. The text above describes the difference between the two methods.

6. SIMPLE HEAT CAPACITY TEST

If the specific heat and density of this model material were constant ($\overline{C_p}$ and $\overline{\rho}$, respectively), then the time that is needed to completely burn through a sample of thickness d would be

$$t_B = \frac{d\,\overline{\rho}\,(\overline{C_p}\,\Delta T + H_s)}{\alpha\,\mathcal{C} - C_L} \quad . \qquad (11$$

where $\mathcal{C}$ is the power of the incoming radiation in W cm^{-2}, α is the absorption coefficient, C_L represents the surface losses, ΔT is the temperature rise from ambient to sublimation of the graphite, and H_s is the heat of sublimation of the graphite fibers and epoxy residue.

The average velocity of recession is

$$v_{r,ave} = d / t_B \qquad (12$$

and the maximum velocity of recession is

$$v_{r,max} = (\alpha\,\mathcal{C} - C_L) / \rho\,H_s \quad , \qquad (13$$

which is the value reached just before burnthrough.

In Figure 5 we show the surface recession velocity as a function of the time of irradiation for the following conditions:

$$d = 0.254 \text{ cm}$$
$$\mathcal{C} = 2.2 \text{ kW}$$
$$\alpha = 0.92$$
$$\rho\,H_s = 1.084 \text{ g/cm}^3 \times 43 \text{ kJ/g} = 46.6 \text{ kJ/cm}^3$$
$$\epsilon_m = 0$$
$$v_{mach} = 0 \quad .$$

These last two conditions (the variables are discussed in Ref. (1) and Ref. (2)) have the effect that there are no reradiative or convective losses at the surface. The other quantity needed is the total energy required to heat the sample to the sublimation temperature of the graphite fibers

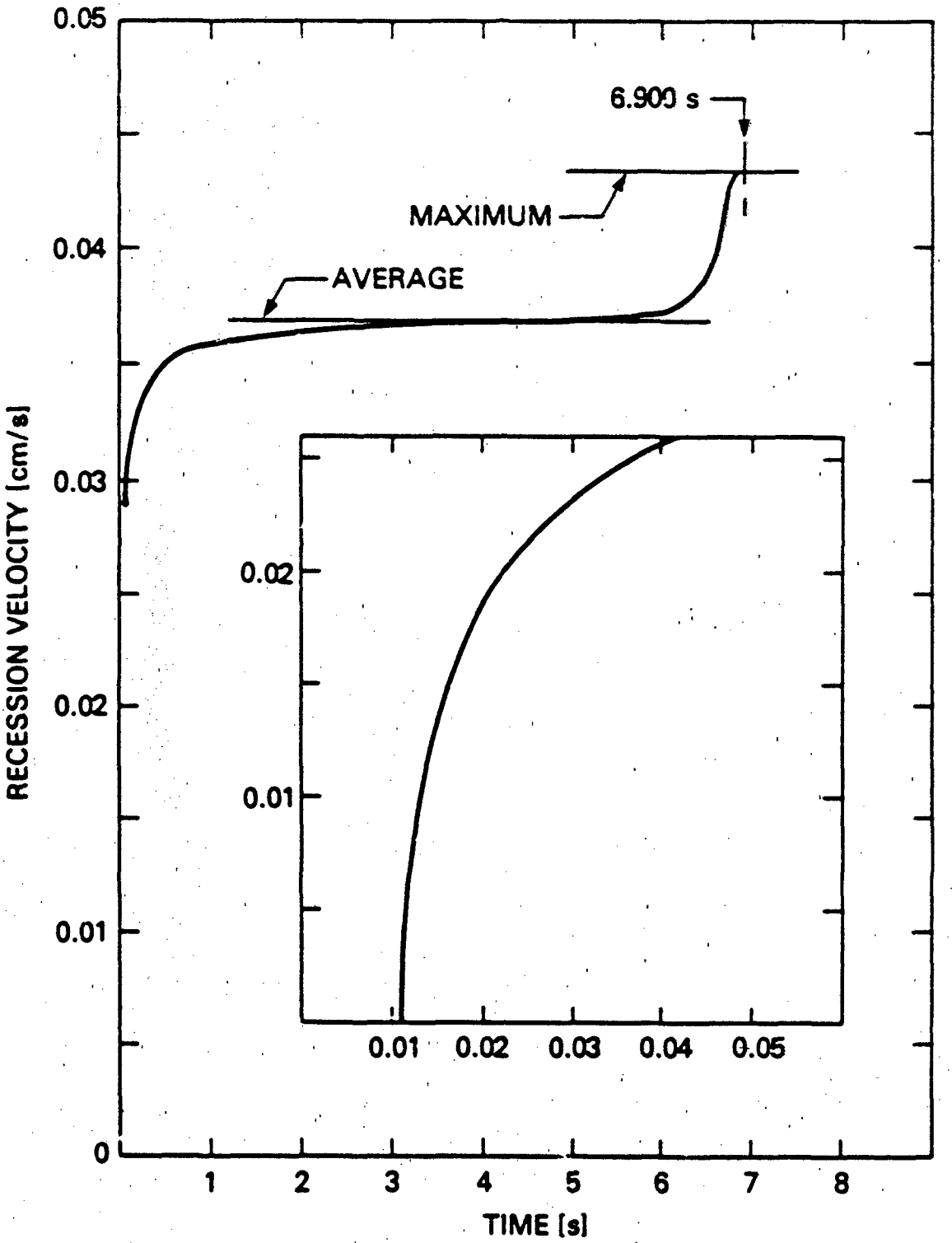

Fig. 5 -- Recession velocity vs. irradiation time for a 0.254 cm thick sample irradiated by 2.2 kW cm^{-2}. (Details of the calculation appear in the text above.)

(T_s = 3316°C). This quantity is calculated in Appendix B; it is 8.3 kJ/cm^2. Upon substituting these values into the expressions for recessional velcity and burnthrough time, we find

$v_{r,ave}$ = 0.0368 cm/sec
$v_{r,max}$ = 0.0434 cm/sec
t_B = 6.500 sec.

To within a millisecond, the code estimates the burnthrough time to be 6.900 sec; the details of the burnthrough process can be seen in Figure 5.

7. COMPARISON WITH THE GRIFFIS, NASUMURA, AND CHANG CALCULATION

The conditions for the GMC calculation with which we compare are

d = 0.254 cm
Q = 2.79 kW/cm^2
α = 0.92
ϵ_m = 0.92
V_{mach} = 0.3 .

For this case we find

$v_{r,ave}$ = 0.0306 cm/s
$v_{r,max}$ = 0.0361 cm/s;

these values are approximate because we used the T=3316°C values of the surfaces losses to estimate the energy absorbed. During the heating process these losses would be somewhat lower.

Figure 6 can be compared with Figure 8 of GMC. There is no substantial difference between the two calculations. The times for the onset of ablation differ by several tenths of milliseconds, but that is due to the improved thermal properties routine, discussed earlier. When I use the GMC routine, I get their value for the onset of ablation.

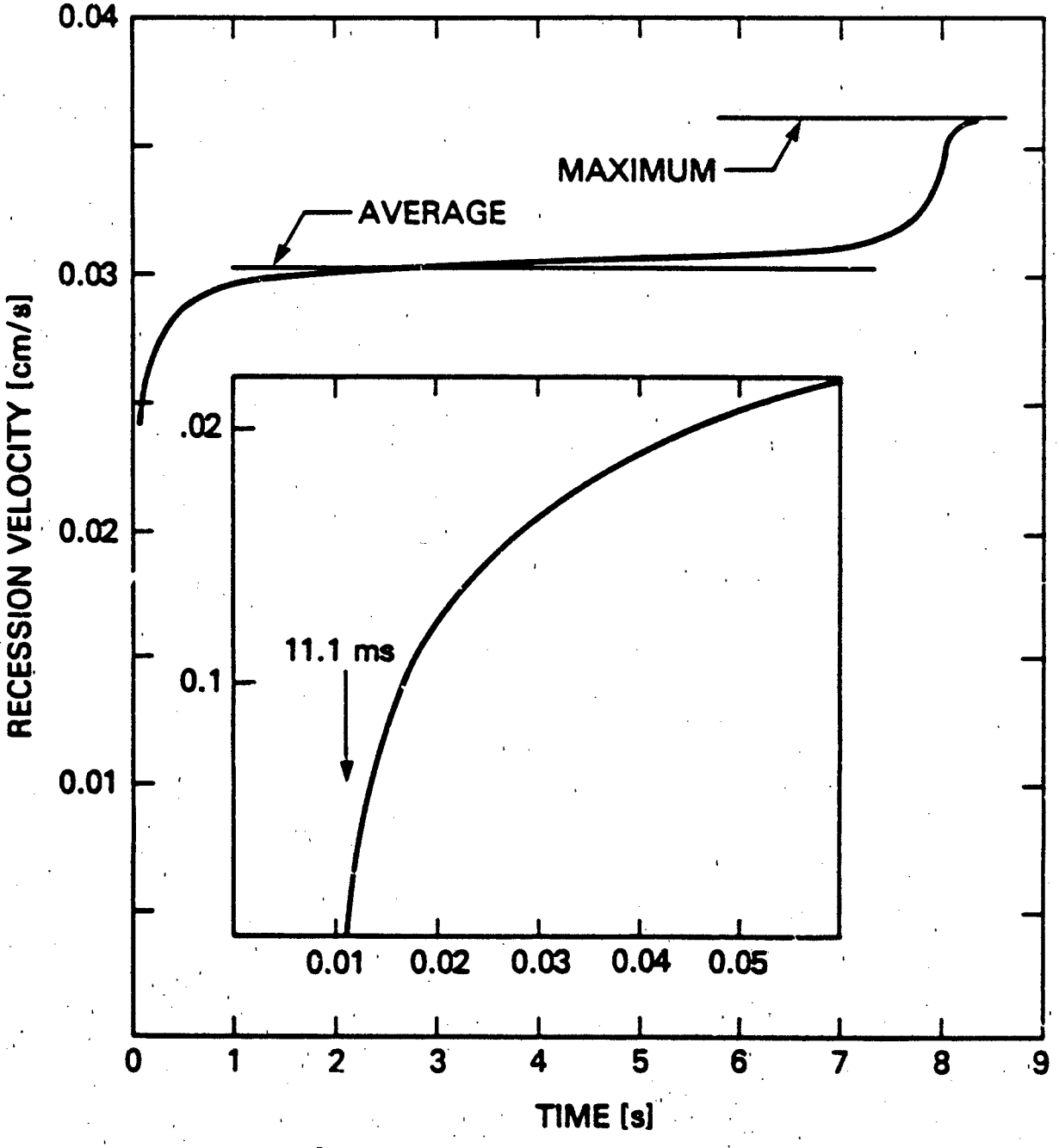

Fig. 6 -- A 2.79 kw/cm^2 CW irradiation for comparison with the equivalent calculation of Griffis, Masumura and Chang. (See the text above for details of the irradiation.)

8. SAMPLE CALCULATION FOR A REPETITIVELY-PULSED IRRADIATION

For the high fluxes that can occur during pulsed irradiations, a plasma can form at the surface of the target material. Once it forms, it absorbs much of the incoming laser radiation and reradiates it over a broad range of wavelengths. We will assume for this model calculation that half of the reradiated energy is absorbed by the graphite epoxy. Figure 7 is a log-log plot of the front surface temperature of the sample as a function of the time from the beginning of each pulse; the results for the first two pulses are shown. Note the rapidity (less than 0.1 μs) with which the surface reaches the carbon fiber ablation temperature.

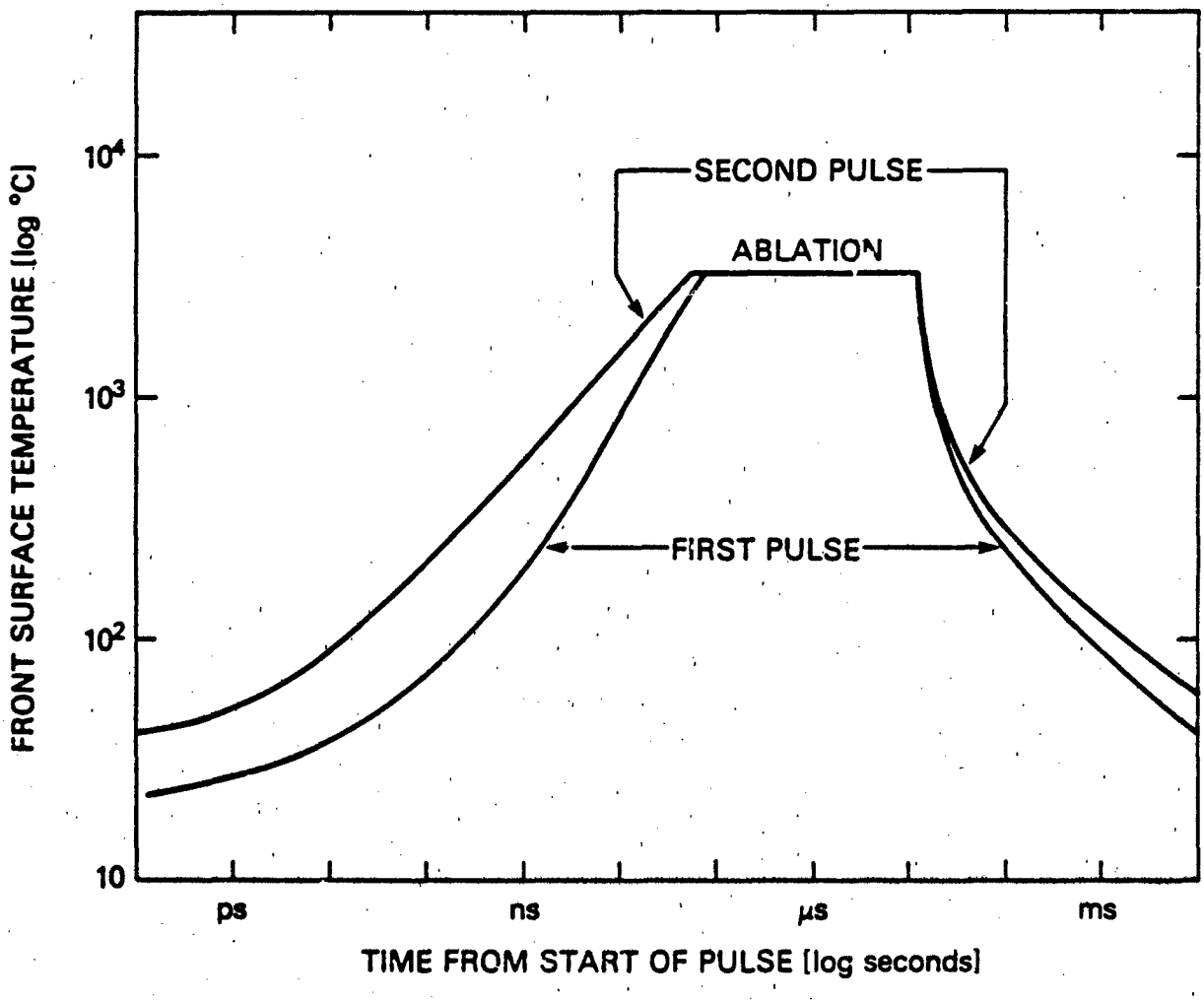

Fig. 7 -- Front surface temperature during a repetitively-pulsed irradiation. (See the text above for details of the irradiation.)

Figure 8 shows the distribution of the remaining energy just before the start of the next pulse. Figure 9 is a graph of the recessional velocity as a function of time during the first two 13 μs pulses. We see that the surface recession rate essentially comes to equilibrium during the first 2-4 μs of each pulse.

The model parameters used in this calculation are

$$d = 0.1 \text{ cm}$$
$$Q = 1.5 \text{ MW/cm}^2$$
$$\alpha = 0.50$$
$$\varepsilon_m = 0.92$$
$$V_{mach} = 0.3$$

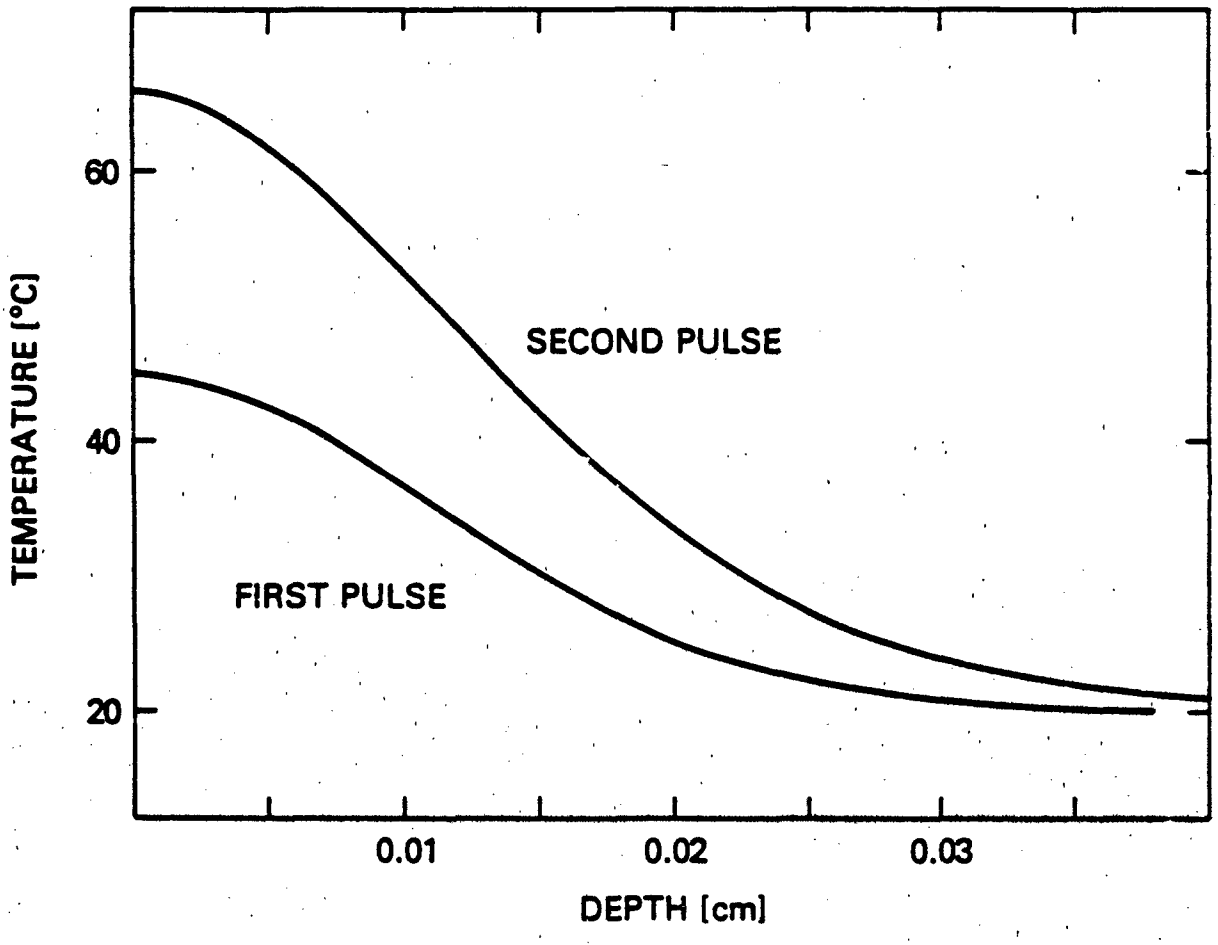

Fig. 8 -- Residual heating: temperature versus depth just before the onset of the next pulse.

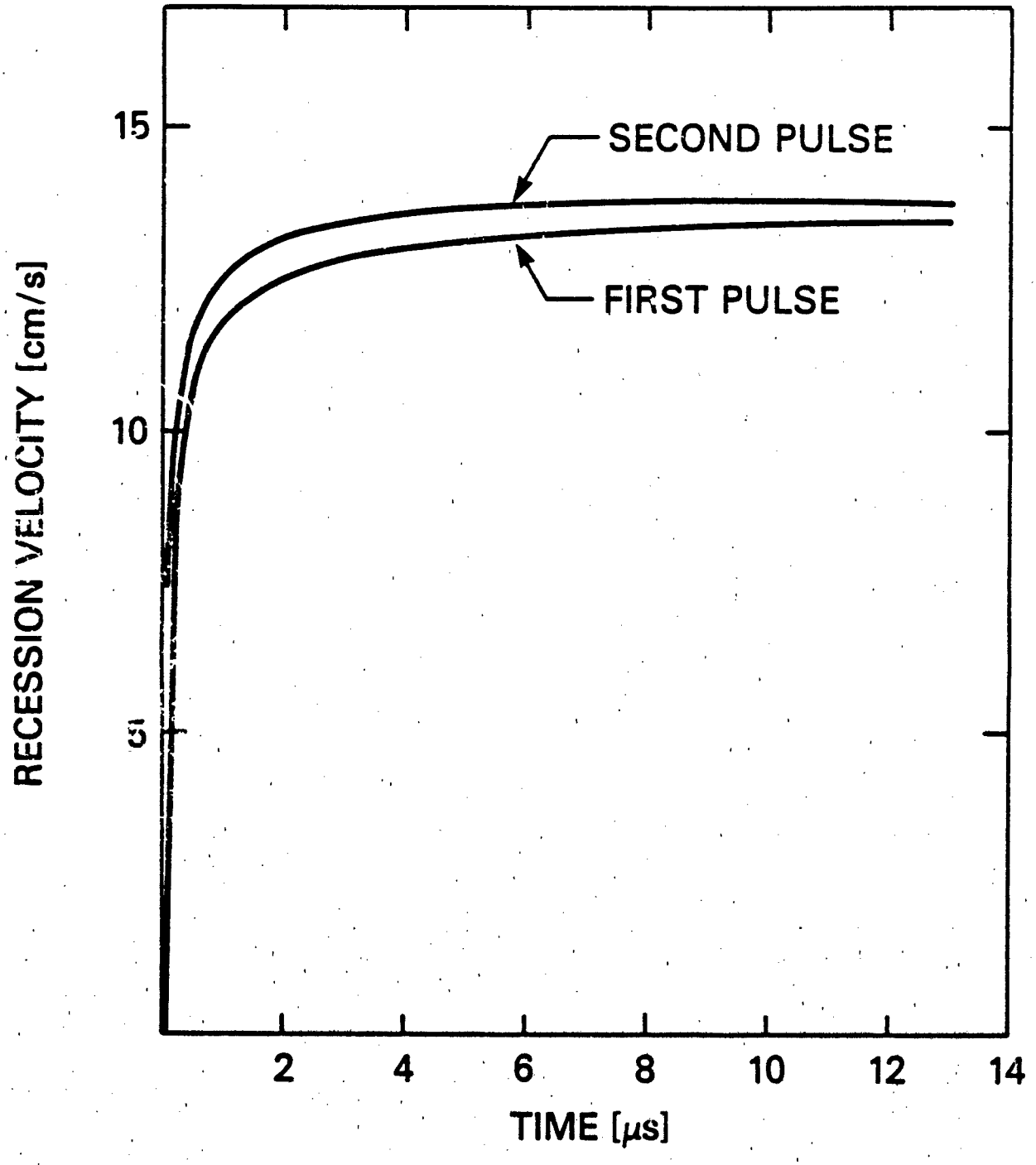

Fig. 9 -- Recession velocity vs. irradiation time for the sample repetitively-pulsed irradiation.

pulse length = 13 μs
repetition rate = 100 p/s .

There is another interesting feature of these pulsed irradiations. For our sample two-pulse irradiation, 19.48 J/cm^2 were absorbed in the composite (≈0.02 J/cm^2 represent the surface losses). At the end of the two pulses, 3.42X10^{-4} cm of the composite had ablated. This required 54.9 kJ/cm^3 X 3.42X10^{-4} cm = 18.75 J/cm^2. Thus 96 per cent of the absorbed energy went to heat and ablate the composite, and only 4 per cent remained in the material. This, at first, surprising result is due to the high incident fluences and the low conductivity of the composite; the surface heats up and ablates much faster than heat can flow into the interior of the material.

9. COMPARISON WITH EXPERIMENTAL REPETITIVELY-PULSED IRRADIATIONS

Much of the data from experimental repetitively-pulsed irradiations is classified, but we can use some of the data of Cozzens and Echols [4]. The parameters for the calculation are

d = 0.2 cm
Q = 625 kW/cm^2
α = 0.92
ε_m = 0.92
V_{mach} = 0.3 .
pulse length = 13 μs
repetition rate = 100 p/s
number of pulses = 100

At this irradiance, we are below the plasma threshold, so we choose the absorption coefficient to be α=0.92; this is the same value used by GMC.

Figures (10)-(12) show the temperatures at the front surface, 8th ply and 15th ply, respectively, for this 16 ply sample. Shown are the calculated values and the experimental values from Reference 4. The front

surface temperatures (Fig. (10)) were measured radiometrically; the other two were measured with thermocouples. The measured front surface temperatures, which were sampled just before the onset of the next pulse, are considerably higher than the calculated values. They are, in fact, off scale on Fig. (10). There is, I think, a simple explanation for this. The code assumes uniform material at the surface, which is slowly eroded by the radiation. In practice, there will be wisps of graphite fibers sticking out that are not in good thermal contact with the body of the material.

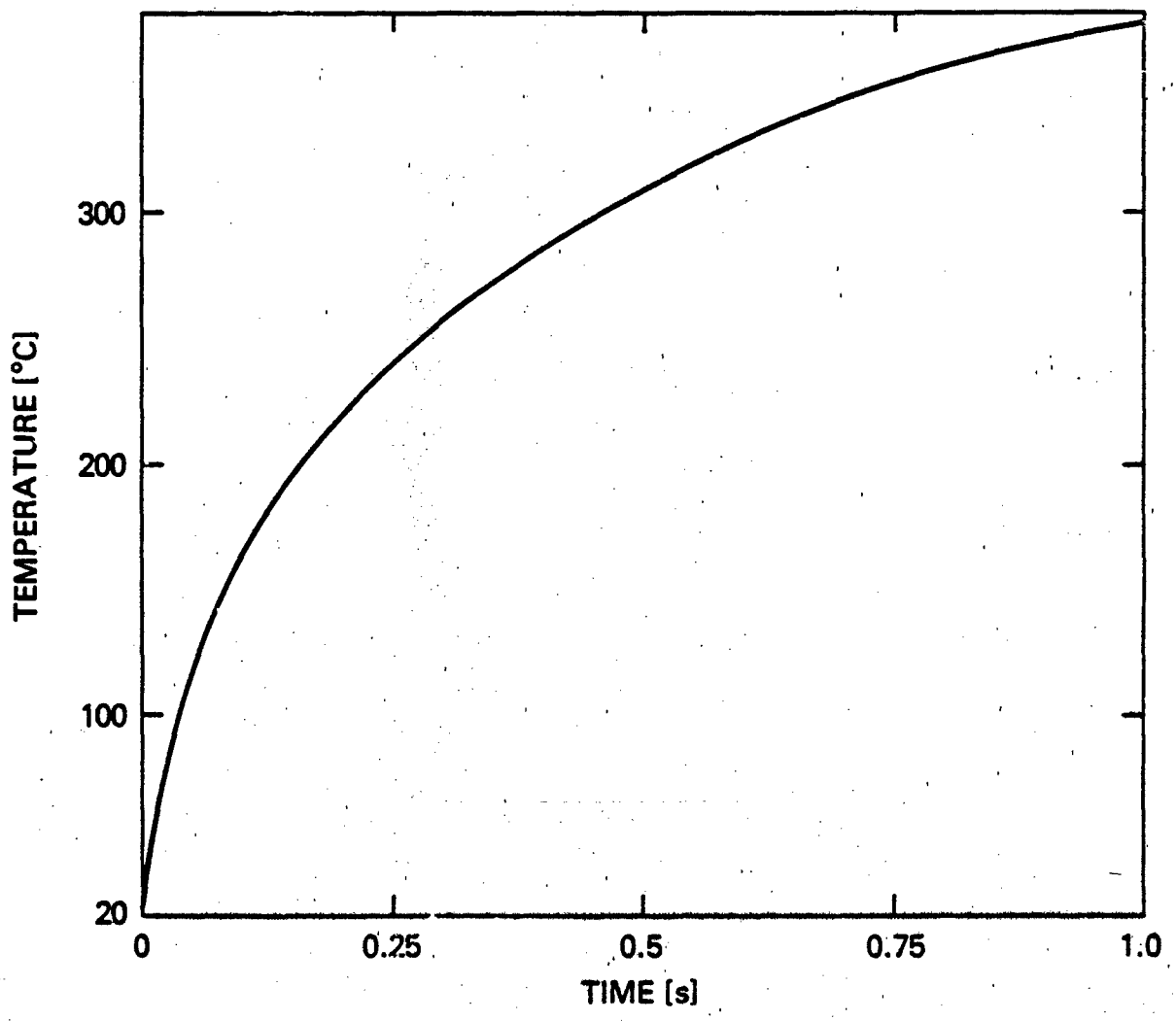

Fig. 10 -- Calculated front surface temperature for a 100 pulse irradiation. (See the text above for details of the irradiation.)

They will retain their heat and continue glowing much longer than if they were in good thermal contact with the bulk material. Consequently, I think the radiometer was picking up the temperature of glowing fibers, not the temperature of the bulk surface.

The temperatures as measured at the 8th and 15th plies are also considerably higher than the calculated values. The simplest explanation for this is that the conductivity used in the calculation is too low. To test this conjecture I arbitrarily increased the low temperature conductivity by doubling the values at 10°C and 343°C. (The values 1.452 and 0.600 in the last column of Table A1 were doubled.) The resulting temperature curves are also shown on Fig. (11) and Fig. (12). We see that there is an improvement in the fit, but given the arbitrary way in which the conductivity was changed, we should take these results only as an indicator.

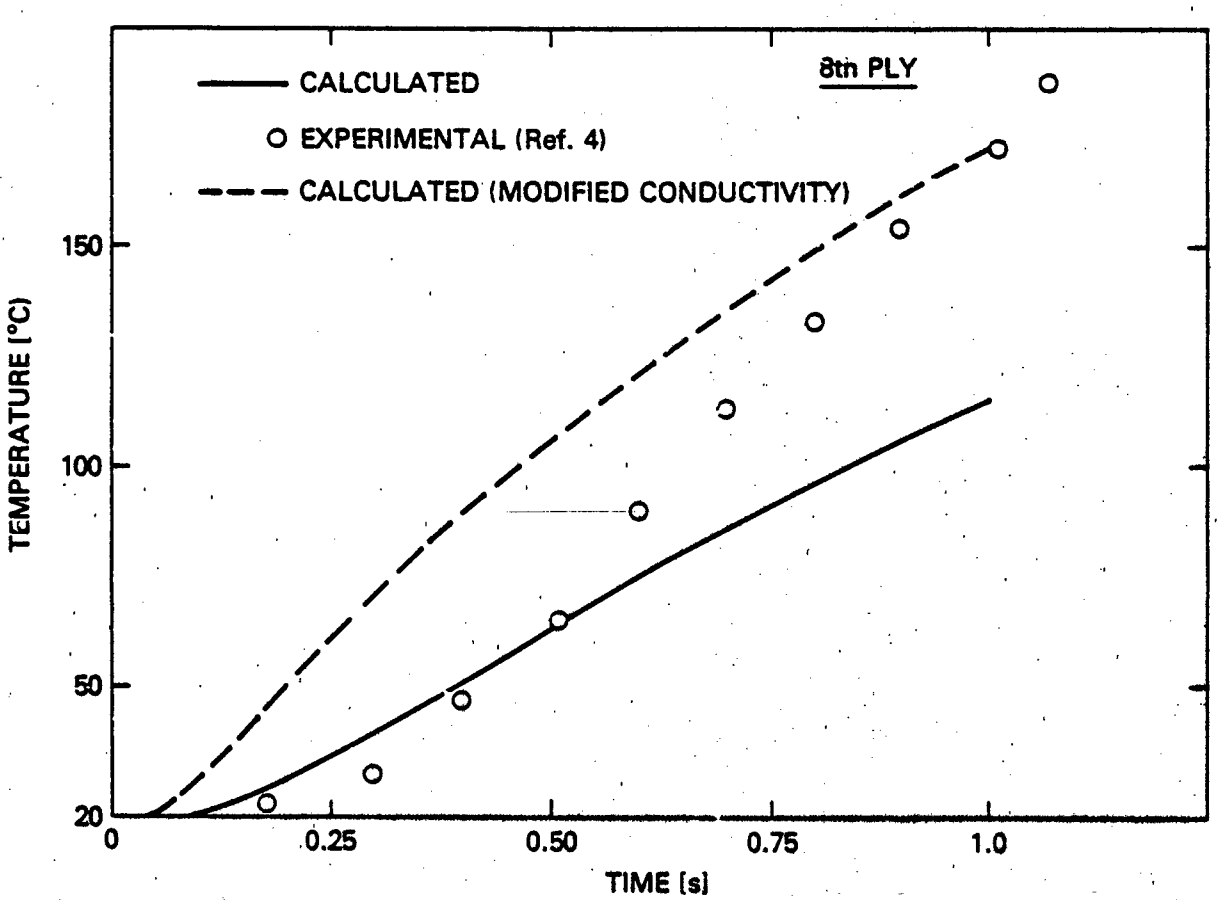

Fig. 11 -- Comparison of calculated vs. measured temperature at the 8th ply for a 100 pulse irradiation. (See the text above for details of the irradiation.)

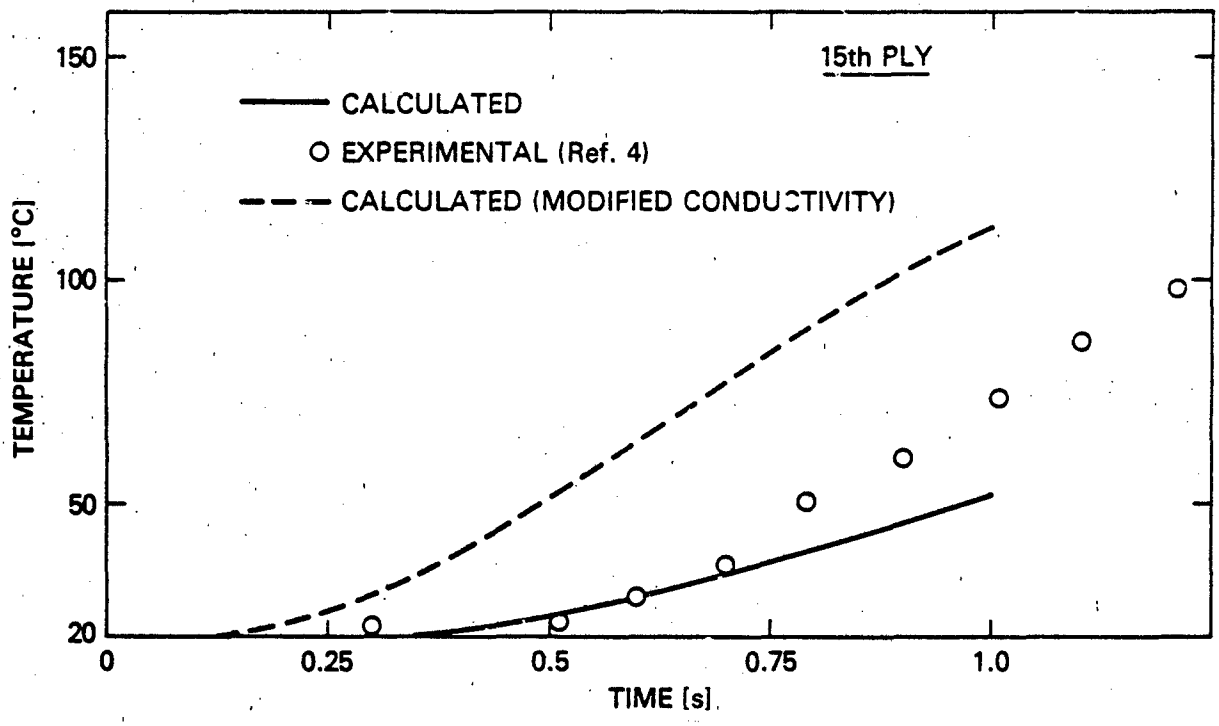

Fig. 12 -- Comparison of calculated vs. measured temperature at the 15th ply for a 100 pulse irradiation. (See the text above for details of the irradiation.)

10. CONCLUSIONS

The discrepancy between the calculated and experimental values is actually worse than pictured, for two reasons. In these calculations, no account is taken of radial heat flow. The experimental irradiation involves a finite sized spot; the temperature rise behind that spot will be less than the calculation for an infinite spot size would indicate. Additionally, the sample in Ref. 4 had a protective coating, which reduced the heat absorbed into the material for several tenths of seconds. These effects each lower the measured temperatures relative to the calculated values. In other words, all of the systematic errors tend to raise the calculated values of interior temperatures, whereas we find them to be lower than the measured values.

The most likely explanation for this discrepancy is that there are errors in the measured (estimated) [3] values for the specific heat and conductivity. Chris Griffis points out [5] that the large peak in the specific heat curve is an attempt to simulate the chemistry of the pyrolyzing epoxy. While this approach may work reasonably well at low fluences and relatively long time-scales, it may not on the short time-scales associated with repetitively-pulsed irradiations.

In any case, further comparisons of calculation and experiment, including any extension of the analysis presented here, must await a second, classified, report [6].

ACKNOWLEDGMENTS

I would like to thank Chris Griffis for giving me a copy of the Griffis, Masumura and Chang code, and all of those authors for discussing the thermal properties of composites with me. Thanks are also due to Bob Cozzens and Bill Echols for giving me their pulsed irradiation data.

REFERENCES

1. C. A. Griffis, R. A. Masumura, and C. I. Chang, "The Response of Graphite Epoxy Composite Subjected to Rapid Heating," NRL Memorandum Report 4479, Naval Research Laboratory, (Washington, D. C.), March 1981. (AD-A096 898)
2. N. P. Hobbs, T. A. Dalton, and R. F. Smiley, "TRAP2-A Digital Computer Program for Calculating the Response of Mechanically Loaded Structures to Laser Irradiation," KA TR-143, Kaman Avidyne (Burlington, Mass.) June 30, 1978. (AD-B076 386)
3. J. F. Menousek and D. L. Monin, "Laser Thermal Modeling of Graphite Epoxy," NWC Technical Memorandum Report 3834, Naval Weapons Center (China Lake, California) June 1979. (AD-D108 417L)
4. R. F. Cozzens and W. H. Echols, private communication.
5. C. A. Griffis, private communication.
6. G. P. Mueller, "Comparison of the Calculated and Measured Thermal Response of Graphite Epoxy Composite to Repetitively-Pulsed Laser Irradiation," NRL Memorandum Report, to be published.

APPENDIX A: THERMAL PROPERTIES OF THE GRAPHITE EPOXY COMPOSITE

1. Thermal Properties of Virgin Material

With one minor modification, we use the Menousek and Monin [3] thermal properties of the graphite epoxy composite.

Table A1

Thermal Properties of Graphite Epoxy Composite

(Taken from Menousek and Monin [3])

[NOTE: The Menousek and Monin version of the conductivity runs from 1.384 W/cm°C at 38°C to 0.173 W/cm°C at 538°C]

TEMPERATURE (°C)	DENSITY (g/cm^3)	SPECIFIC HEAT (J/g°C)	CONDUCTIVITY (w/cm°C)
10	1.506	1.254	0.01452
343^-	1.506	2.093	0.00600
343^+	1.506	5.024	0.00600
510^-	1.506	4.899	0.00173
510^+	1.084	1.591	0.00173
3316	1.084	2.512	0.00173

In order to improve the numerical stability of their code, GMC modified the Menousek and Monin properties as listed in Table A2.

2. Thermal Properties of Thermally Cycled Material

The large changes in the thermal properties between 300°C and 500°C are due the chemical reactions in and the final sublimation of the epoxy. Above 510°C we assume that only the graphite fibers and some residue of the epoxy remain. Consequently, when a portion of the material that was heated above 510°C cools, its thermal properties are different due to the loss of the epoxy. Table A3 lists the properties for this case. Any portion that has not reached 510°C is assumed to retain all of its epoxy and to still have the properties of the virgin composite. These properties are the same

whether one starts with the original Menousek and Monin properties, my modification of them, or the GMC modification.

Table A2
Thermal Properties of Graphite Epoxy Composite
(As used by Griffis, Masumura, and Chang)

TEMPERATURE (°C)	DENSITY (g/cm^3)	SPECIFIC HEAT (J/g°C)	CONDUCTIVITY (W/cm°C)
10	1.506	1.254	0.01384
329	1.506	2.056	0.00651
357	1.506	5.007	0.00587
496	1.506	4.902	0.00269
524	1.084	1.593	0.00228
566	1.084	1.607	0.00206
621	1.084	1.625	0.00187
704	1.084	1.652	0.00179
816	1.084	1.689	0.00173
3316	1.084	2.508	0.00173

Table A3
Thermal Properties of Graphite Epxoy
That Has Been Heated above 510°C

TEMPERATURE (°C)	DENSITY (g/cm^3)	SPECIFIC HEAT (J/g°C)	CONDUCTIVITY (W/cm°C)
10	1.084	1.427	0.00173
3316	1.084	2.506	0.00173

APPENDIX B: CUMULATIVE HEAT CAPACITY

In order to calculate the average recession velocity, we need to know the energy required to heat the graphite epoxy from ambient (20°C) to the sublimation temperature of the graphite (3316°C). Within each region for which the density and specfic heat vary linearly, the cumulative heat capacity is

$$D(T_2,T_1) = \int_{T_1}^{T_2} dT\, \rho(T)\, C_p(T) \qquad \text{(B1}$$

$$= (T_2 - T_1)\,[2\rho_1 C_{p1} + \rho_1 C_{p2} + \rho_2 C_{p1} + 2\rho_2 C_{p2}] \quad . \qquad \text{(B2}$$

Table B1 gives the value of D for each region as well as the cumulative value from ambient to sublimation.

Table B1
Cumulative Heat Capacity of Graphite Epxoy
(Based on the Properties in Table A1)

TEMPERATURE	INTERVAL HEAT CAPACITY $D(T_i,T_{i-1})$	CUMULATIVE HEAT CAPACITY $D(T_i,20°C)$
(°C)	(J/cm^3)	(J/cm^3)
20	0	0
343	821	821
510	1248	2069
3316	6240	8309

The equivalent value for the material after it has been heated above 510°C is $D(3316°C,20°C)=7037\ J/cm^3$.

When one uses the CMC version of the thermal properties, one obtains the following values for the cumulative heat capacity.

Table B2

Cumulative Heat Capacity of Graphite Epxoy

(Based on the Thermal Properties in Table A2)

TEMPERATURE	INTERVAL HEAT CAPACITY $D(T_i, T_{i-1})$	CUMULATIVE HEAT CAPACITY $D(T_i, 20^\circ C)$
(°C)	(J/cm^3)	(J/cm^3)
20	0	0
329	770	770
357	149	919
496	1037	1956
524	120	2076
566	73	2149
621	96	2245
704	147	2392
816	203	2595
3316	5688	8283